



# An Experimental Approach to Image the Rotated Straight Baseline for the Water Sliding Angle Measurement of a Rough Surface

Teeranan Nongnual<sup>1,\*</sup>, Nontakorn Damnong<sup>2</sup>, Sineenart Srimongkol<sup>3</sup>, Sirikhun Phanrangsee<sup>4</sup> and Takat Benjalersyarnon<sup>5</sup>

<sup>1</sup> Department of Chemistry, Faculty of Science, Burapha University, Thailand  
e-mail : [teeranan.no@buu.ac.th](mailto:teeranan.no@buu.ac.th)

<sup>2</sup> Department of Adult Nursing, Faculty of Nursing, Burapha University, Thailand  
e-mail : [nontakorn@buu.ac.th](mailto:nontakorn@buu.ac.th)

<sup>3</sup> Department of Mathematics, Faculty of Science, Burapha University, Thailand  
e-mail : [sineenart@buu.ac.th](mailto:sineenart@buu.ac.th)

<sup>4</sup> School of Liberal Arts, Walailak University, Thailand  
e-mail : [tsirikhu@wu.ac.th](mailto:tsirikhu@wu.ac.th)

<sup>5</sup> Department of Mechanical Engineering, Faculty of Engineering, Rajamangala University of Technology Rattanakosin, Thailand  
e-mail : [takat.ben@rmutr.ac.th](mailto:takat.ben@rmutr.ac.th)

**Abstract** Water sliding angle is one of common parameters that indicates the hydrophobicity and water repellency of a material surface. Drop shape analysis technique was normally used to measure the sliding angle by video imaging a water drop rolling off the rotated surface. The typical baseline of a flat surface was determined from consecutive drop shape images, resulting the relationship between the tilt angle against the acquisition time. To apply this method for a rough surface such as paper, cloth, porous material, or non-woven fabric, an additional experimental setup was introduced in this work to reduce the difficulties in the linear regression calculation of the wavy data points. The material was attached to a flat surface reference, which was imaged and extracted to a rotated straight baseline. In addition, the imaging latency of the camera and the rotation lag time of the angular rotor were suppressed by monitoring the image brightness that was synchronized to the rotation duration. The sliding angle was then precisely calculated by using the computer algorithms written in MATLAB. It was found that our proposed experimental approach and the computational algorithms yielded such accurate and reliable water sliding angle of the rough surface, significantly different from those calculated by the conventional setup. These results suggested that our method could be useful as a handy tool to study the water repellency of advanced materials.

**MSC:** 68U10; 90C90; 62J05

**Keywords:** water sliding angle; rough surface; baseline reference, water repellency

---

Submission date: 26.04.2021 / Acceptance date: 19.07.2021

---

\*Corresponding author.

## 1. INTRODUCTION

To indicate the hydrophobicity and the water repellency of a material surface, typical water contact angle and water sliding angle have been widely reported in previous studies [4]. The contact angle was defined by the angle between a liquid-vapor interface and a solid surface [3]. Whereas the sliding angle or the roll-off angle is the minimum tilt angle of the surface that a water drop rolls off. Although the contact angle is consistent with the sliding angle thus the contact angle has been solely reported, the sliding angle could provide additional information on the surface properties. The water sliding angle particularly expressed the unique characteristics and advanced applications of materials such as superhydrophobic coating [7], self-cleaning surface [1], separation of multiple-phase mixture [8], or chemical-selective membrane [2].

The water sliding angle was typically measured by using a drop shape analysis technique. This method was performed by taking a video image of a water drop placed on a material surface while the sample stage was tilting to a defined angle. The cradle could be tilting manually or automatically with constant inclination speed available in advanced instruments. After the images were analyzed by specific software (Kruss, Germany) [5], three-phase points at the interface of solid, liquid and surrounding vapor phase were located at both sides of the drop. The sliding angle was defined as the angle at which the three-phase point displacing by 40 pixels. Tracking the three-phase point could be complicated in the image-processing step. A simple and precise method with custom computational algorithms was thus introduced in this work to measure the sliding angle of material surface.

Herein, an experimental procedure and a computational calculation step will be explained to measure the sliding angle of a rough surface. The rotated baseline of the rough surface was substituted by a flat glass slide to reduce the difficulties in the computational calculations of a linear regression. In addition, to avoid a calculation deviation caused by the latency of the device, the rotation period was synchronized to the imaging duration.

## 2. MATERIALS AND METHOD

Typical white fabric made from cotton fiber was purchased from a local textile market in Chonburi, Thailand without pre-washing. The rugged and hairy surface of the cotton fabric was likely due to the disordered cellulose fibers thus it was used as a rough-surface material in this work. The cotton fabric was cut to a rectangle of about  $1 \times 2$  inch<sup>2</sup> and was attached to a glass slide. The glass slides (CAT. No. 7105) were purchased from Sail Brand.

The sliding angle of the fabric was measured by video-imaging of a water droplet with the volume of 30  $\mu$ L placed on the surface using the drop shape analyzer DSA-30 (Kruss, Germany). As the method is based on gravity, the sliding angle undoubtedly depends on the volume of the droplet. Thus, the same drop size was used in this work for comparison. Experimental procedures of the instrument were controlled by using the DSA-4 software. The tilting stage PA4240 was installed at the sample base, which was placed between an illuminator and a video-recording camera. The camera Stingray F046B IRF was operated at the camera angle of zero degree with a 25-Hz framerate. The sample base was rotated from zero to 90 degrees with a rotor angular speed of 0.1 degree per frame and a total video recording time of about 36 s.

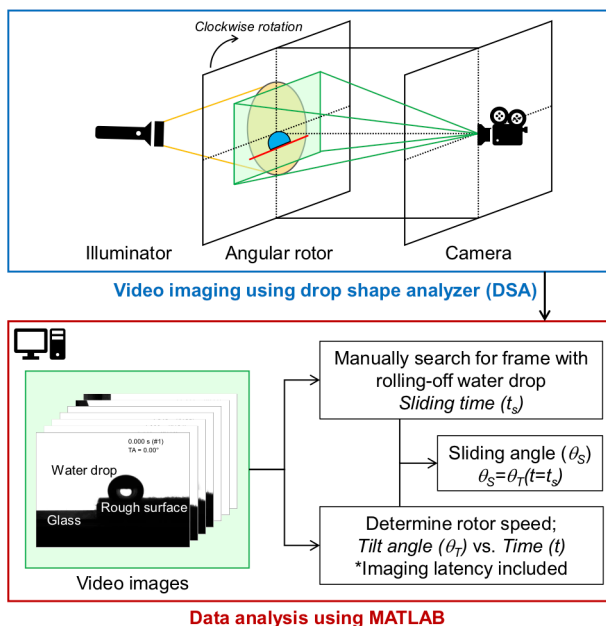


FIGURE 1. Schematic illustration of the experimental steps and computational calculations of sliding angle by using drop shape analysis method

The experimental setup and corresponding computational calculations as shown in Figure 1 were discussed in this work to describe the measurement of the sliding angle of a rough surface. The roughness of the cotton fabric could deliver such difficulties in the calculation of the rotated baseline. Alternatively, attaching the fabric to half of the glass slide might significantly correct the rotated linear baseline of the flat glass and decrease the computational time during the iterations. The resulting sliding angle from the modified setup will be discussed and statistically compared to the conventional method. Moreover, the rotor speed that shows the relationship between the tilt angle ( $\theta_T$ ) and the recording time ( $t$ ) could be deviated by the imaging latency. Therefore, the synchronization between the camera and the angular rotor will be determined by monitoring the rotation period with corresponding video images.

### 3. RESULTS AND DISCUSSION

A small water droplet with the volume of  $30 \mu\text{L}$  was ejected and placed on a rough surface of the cotton fabric, which was attached to a glass slide. The roughness of the surface clearly shown that the baseline might be poorly fit to a linear model so an alternative procedure was proposed in this work. The fabric was not covered the slide entirely thus there could have a space left for the bare slide as shown in Figure 2. The perfect flat of the glass could be clearly considered as a linear rotated baseline. The sample stage was connected to an angular rotor of the drop shape analyzer and was consecutively imaged by using a camera while the sample stage was being rotated to 90 degrees.

The water drop, the glass slide, and the rough surface were simultaneously captured as in the dark area of the image while the illuminated background was in white area.

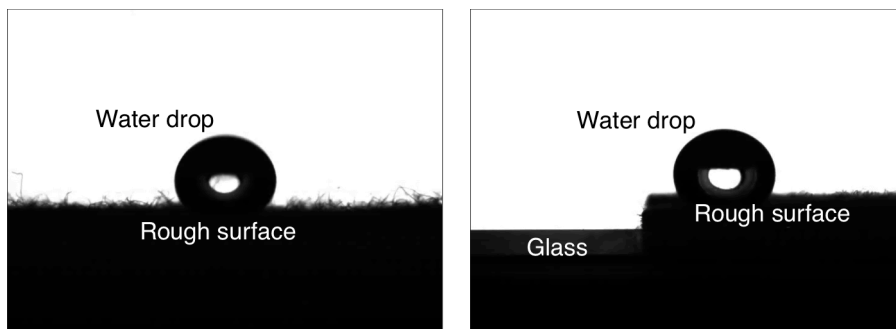


FIGURE 2. An image of a water drop on the rough surface of the cotton fabric that entirely (left) or partially (right) covered a glass slide.

The boundary between these colors was extracted for each consecutive image by using a partial area effect technique as an image-processing function written in Matlab available online [6]. The resulting edge lines of the selected data without and with a flat glass slide are shown in Figure 3. The interval between the edges was set at 30 frames to present somewhat clear and distinguishable illustration.

Due to the roughness of the cotton fabric, the extracted boundary between the object and the background was obviously not straight. This significantly caused the difficulties in the computational calculations of the linear regression. Thus, the tilt angle of the incorrect line related to the baseline was not accurate. An additional experimental procedure in this work will be explained to provide a straight rotated baseline during the sliding angle measurement of the rough surface.

The straight edge line was chopped at the first 100 pixels along the  $xy$  axes. This line obviously belonged to the flat area of the glass slide that was placed under the sample and shown on the left of the image. The crop range was adjustable to selectively cover the flat area by using our written Matlab script that seeks for the rapid change of the image brightness along each axis. The left part of the edges was highlighted in red color outside the blue box. The tilt angle will be calculated at each image by using the tangent method corresponding to two cropped rotated baselines.

Electronic and mechanical devices particularly the mechanical angular rotor and the camera embedded in the drop shape analysis instrument in this work commonly have a significant time delay known as latency. It was likely due to, for instance, triggering, processing commands, or transferring signal. Thus, the camera was pre-adjusted to take a video image longer than the given parameters to cover the entire period of the rotation. The total recording time of the selected image was 39.7 s corresponding to 993 frames at a framerate of 25 Hz. To eliminate the accumulated latency, the exact time period of the rotation will be synchronized by calculating constant brightness of the images at the last few seconds.

The pixels of the video image were recorded in an 8-bit grayscale, of which black is set zero, white is 255, and the grey shades fall in between. The summation of the grayscale number of entire pixels in each image was calculated as the image brightness. The pixel size of the selected image was  $708 \times 528$ , yielding the brightness of about  $9.5 \times 10^6$  of a complete white image. While the sample was being rotated by the angular rotor, the

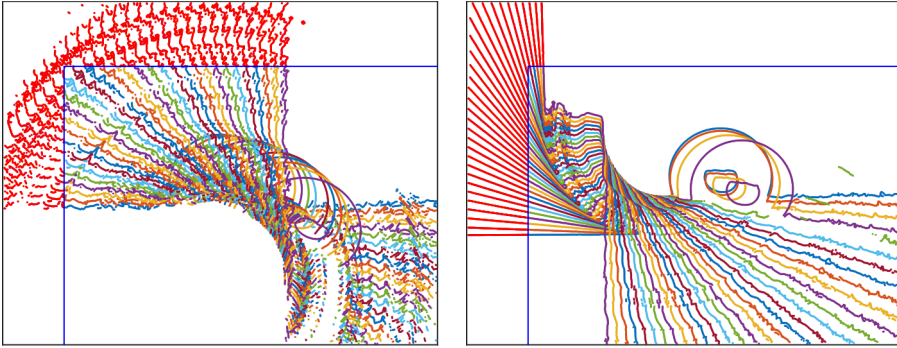


FIGURE 3. The boundary between white and dark pixels of the images taken by the conventional method (left) and our proposed experimental setup (right).

dark area of the stage could be seen more or less in the image depending on the camera border at different tilt angle.

The image brightness in this case was linearly increasing at the late time as shown in Figure 4. The brightness was suddenly flat at 37.700 s or frame number 943, showing the final time ( $t_f$ ) of the rotation with stopped sample stage. The camera extended to capture the image for a few seconds to cover the latency. The  $t_f$  was initially estimated by using the functions in MATLAB; *smooth* to remove small bumps and *islocalmax* with ‘*flatselection*’ set at ‘*first*’ to find the first point of the local flat maxima regions. The brightness data was split into two parts, which are a few seconds before and after the initial guess of  $t_f$ . They were fit to a linear function then the corrected  $t_f$  was calculated by the intersection of these two lines. The images recorded after the  $t_f$  will be removed to avoid the latency compensation of the camera.

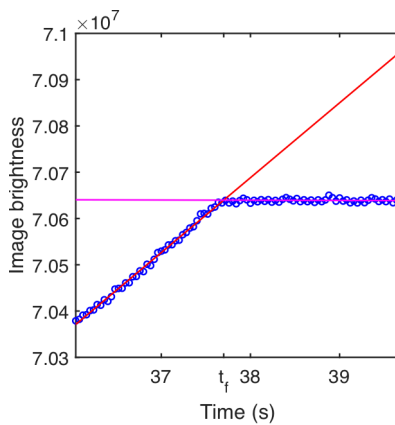


FIGURE 4. The image brightness at the late acquisition time with two fitted linear functions crossed at the final time of the angular rotation.

The cropped edge lines corresponding to the video images from the first frame to the frame at  $t_f$  were chosen. The tilt angle ( $\theta_T$ ) of each image expressing the angular rotation

speed was calculated by the tangent method of the rotated baselines relating to the first edge line at the original position following an equation,

$$\theta_T = \tan^{-1} \left( \frac{m_i - m_0}{1 + m_i m_0} \right), \quad (3.1)$$

where  $m_0$  is the slope of the baseline at the first frame and  $m_i$  is the slope of rotated edge line at frame number  $i$ . The calculated tilt angles were plotted against the corresponding time ( $t$ ) as shown in Figure 5. The data were fitted to a linear function,

$$\theta_T = mt + c, \quad (3.2)$$

where the slope  $m$  is the angular speed of the rotor and the constant  $c$  refers to a trigger latency.

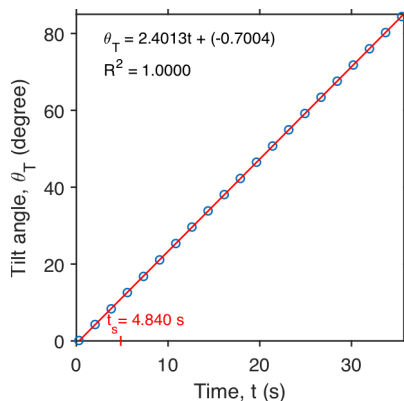


FIGURE 5. The plot of the tilt angle of the angular rotor against the acquisition time of the camera.

The selected data yielded a linear function of  $\theta_T = 2.4013t + (-0.7004)$  with an  $R^2$  of 1.0000. The slope of 2.4013 degrees per second can be converted to about 0.1 degree per frame at the framerate of 25 Hz. The regression predictions perfectly fit the data shown that the angular rotor was smoothly rotating at a constant speed. The angular speed was pre-adjusted in the software with the rotor unit speed of 1.5 unit per second and the constant rotor angular speed of 0.64 unit per degree.

According to the fitted linear equation, the  $x$ -intercept point of 0.29 s was calculated by the minus of  $y$ -intercept over the slope, which shown the lag time due to mechanical latency of the rotor. The camera took an image for a moment before the rotor started to rotate by the computer command. The trigger latency at the beginning and the camera capture extension at late time were clearly determined by the proposed synchronization to avoid any calculation errors in the determination of the tilt angle and angular speed of the rotor.

The experimental modification of the sample imaging of the flat surface reference yielded a perfect linear relationship as a standard curve of the tilt angle with linear rotated baselines. In addition, the smooth glass surface decreased the computational time for the iteration in linear regression. Thus, imaging a glass surface as the rotation reference significantly enhanced computational calculation of the sliding angle of rough surface. The

sliding time will be then calculated and inserted into the equation to calculate the sliding angle.

The sliding time ( $t_s$ ) was estimated by manually pick an image that shows the sudden removal of the water drop. Another computational approach from our lab to calculate the  $t_s$  will be reported elsewhere. The images of the water drop rolling off the surface are shown in Figure 6 along with the edge lines. The drop rapidly jumped out from the surface as shown in the frame number 121 to 122. The resulting  $t_s$  was 4.840 s at frame number 122 with a tilt angle of 11.55 degrees. The sliding time was inserted in the fitted linear equation yielding a sliding angle ( $\theta_S$ ) of 10.9 degrees. It should be noted that the reported water sliding angle was somewhat similar to the tilt angle calculated from one image. In fact, the sliding angle estimated by the proposed experimental approach was more accurate due to the removal of accumulated latency by the device synchronization.

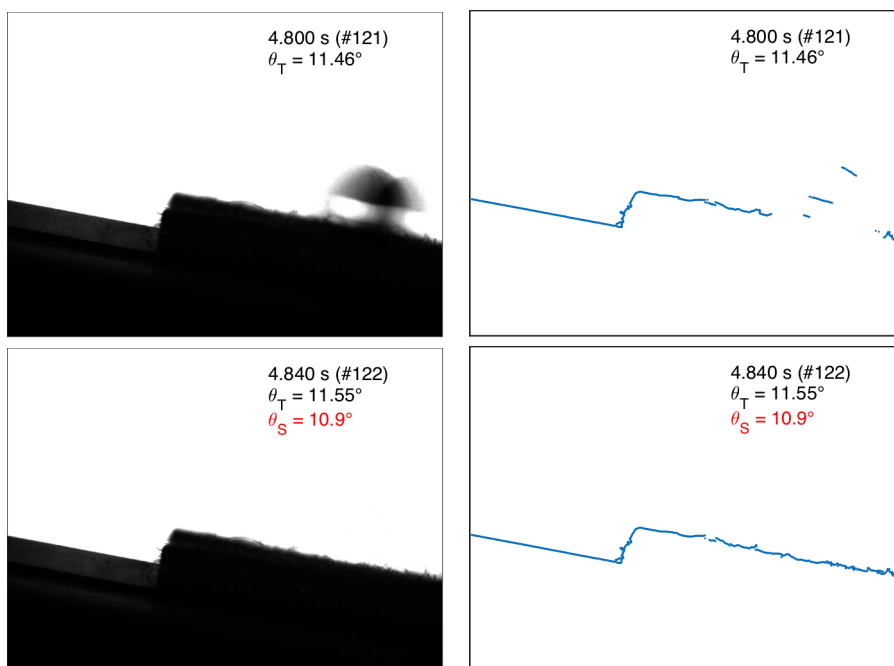


FIGURE 6. The drop shape images of the rolling-off water drop at frames number 121 and 122 with the corresponding boundary line.

An independent-samples t-test was conducted to compare the resulting water sliding angle of the cotton fabric surface by using two different experimental setups. The rotated baseline can be calculated by the conventional method that takes an image of a water drop on entire rough surface, and our proposed method that records a part of the rough surface together with a flat glass slide. The proposed method was expected to yield such a reliable result and reduce computational calculation time. It was found that there was a significant difference in the sliding angle results calculated by using the conventional method with the mean of 30.1 degrees and the variance of 178.0 ( $n = 10$ ), and the proposed method with the mean of 10.9 degrees and the variance of 2.7 ( $n = 10$ );  $t(9) = 2.2622$ ,  $p = 0.0014$ . These results suggest that the experimental setup has an effect on

the calculations of the rotated baseline and the sliding angle. In addition, the coefficient of determination ( $R^2$ ) of the linear regression was 1.0000 for the tilt angle against time calculated by our proposed method due to the flatness of the glass slide. Whereas the  $R^2$  was in the range of 0.7805 to 0.9953 for those calculated by the conventional method due to the roughness of the surface. Specifically, our proposed experimental method was practical and provided such reliable and accurate sliding angle results.

#### 4. CONCLUSION

The experimental approach was proposed in this work to precisely estimate the water sliding angle of a rough surface. The rotated baseline was calculated at the flat line of the glass slide, resulting a standard curve of the tilt angle. To avoid the error from the latency, the synchronization of the angular rotor and the camera was performed by monitoring the change of the image brightness. It was found that the edge line of the rough surface could not precisely be predicted by linear regression. Contrarily, a flat glass slide shown at the left of an image was perfectly fitted to a linear function as expected. The corresponding tilt angle was precisely determined by the tangent method that related the rotated baseline to the original position. The sliding angle of the rough surface sample was precisely estimated by our proposed method, which was significantly different to the conventional method. The results suggest that the practical experimental approach and fast computational scripts in this work might be useful for a study of the hydrophobicity or water repellency of such advanced materials with a rough surface.

#### ACKNOWLEDGEMENTS

The authors gratefully acknowledge the use of services and facilities from the Department of Mathematics and the Department of Chemistry, Faculty of Science, Burapha University. We also thank Ms. Prakaiwan Kotchapun for the assistance in our laboratory. The present study was supported by a research grant from the National Science and Technology Development Agency (Grant number FDA-CO-2563-12485-TH).

#### REFERENCES

- [1] B. Chen, J. Qiu, E. Sakai, N. Kanazawa, R. Liang, H. Feng. Robust and superhydrophobic surface modification by a “paint + adhesive” method: Applications in self-cleaning after oil contamination and oil-water separation, *ACS Appl. Mater. Interfaces* 8 (2016) 17659–17667.
- [2] C. Chen, D. Weng, S. Chen, A. Mahmood, and J. Wang, Development of durable, fluorine-free, and transparent superhydrophobic surfaces for oil/water separation, *ACS Omega* 4 (4) (2019) 6947–6954.
- [3] T. Huhtamki, X. Tian, J. T. Korhonen, Robin H. A. Ras, Surface-wetting characterization using contact-angle measurements, *Nat. Protoc.* 13 (2018) 1521–1538.
- [4] S. Li, J. Huang, Z. Chen, G. Chen, and Y. Lai, A review on special wettability textiles: theoretical models, fabrication technologies and multifunctional applications, *J. Mater. Chem. A* 5 (2017) 31–55.
- [5] F. Thomsen, T. Winkler, Roll-off of sliding angle and dynamic contact angles, *Proceedings of the Kruss Technical Note TN317e* (2012) 1–4.



- [6] A. Trujillo-Pino, K. Krissian, M. Alemn-Flores, D. Santana-Cedr es, Accurate subpixel edge location based on partial area effect, *Image and Vision Computing* 31 (1) (2013) 72–90.
- [7] C. Zhou, Z. Chen, H. Yang, K. Hou, X. Zeng, Y. Zheng, J. Cheng, Nature-inspired strategy toward superhydrophobic fabrics for versatile oil/water separation, *ACS Applied Materials & Interfaces* 9 (10) (2017) 9184–9194.
- [8] X. Zhou, Z. Zhang, X. Xu, F. Guo, X. Zhu, X. Men, B. Ge, Robust and durable superhydrophobic cotton fabrics for oil/water separation, *ACS Applied Materials & Interfaces* 5 (15) (2013) 7208–7214.